# KINETIC AND EQUILIBRIUM DATA OF GASES IN GLASS MELTS

MARCELA JEBAVÁ, LUBOMÍR NĚMEC, JAROSLAV KLOUŽEK

*Laboratory of Inorganic Materials*
*Joint Workplace of the Institute of Inorganic Chemistry of the Academy of Sciences of the Czech Republic*
*and the Institute of Chemical Technology Prague*
*Technická 5, 166 28 Prague, Czech Republic*

E-mail: nemec@iic.cas.cz

Submitted June 23, 2004; accepted September 1, 2004

**Keywords:** Mathematical model, Glass, Bubbles, Gas diffusion

*The method of the high temperature observation with subsequent bubble analysis by mass spectrometry was used for the determination of physical constants of gases dissolved in glass melts. The procedure arises from the mathematical model of the bubble behaviour in glass melt, namely the bubble size and composition developments. These two time dependences were also experimentally measured and used for the acquisition of diffusion coefficients, physical solubilities and actual concentrations of* $CO_2$*,* $N_2$ *and Ar in the TV glass at temperatures 1300°C and 1400°C.*

## INTRODUCTION

Solubility and diffusion of gases in glass melts are associated with several significant glass areas such as glass structure, glass permeability for gases or glass technology. The interactions between glass melts and gases influence particularly the melting process of glass and resulting glass colour. The presence of gases in glass melts has both chemical and physical nature, but in most cases the physical solubility of gases and their diffusion coefficients in melt are data needed for quantitative description of bubble behaviour in glass melts and oxidation-reduction interactions of gases in glass melts determining both refining and glass colour, as well as glass heating and its workability. The application of rather complicated mathematical models of the melting process thus considerably depends on the accuracy of physical solubility and diffusion coefficients of appropriate gases in glass melts.

The methods of diffusion coefficient measurement in glass melts are mostly based on following the interaction between defined volume of gas and glass melt. Bubbles containing the examined gas or diffusion vessels with gas, immersed in the melt, were applied to measure the gas volume dissolution in the melt [1,2]. To acquire the appropriate diffusion coefficient, the physical solubility of the gas in the melt was nevertheless needed. No other gas was allowed in the melt to prevent its impact on mass transfer. The physical solubility of gases in glass melts is in relation to the free volume in the glass structure, available for molecules of dissolved gas [3]. The values of the Ostwald's absorption coefficient of $H_2$, He, Ne and $O_2$ range from 0.01 to 0.03 [4,5] and are only slightly dependent on temperature. Then the approximate value of gas solubility in glass melt varies in the range of tenths of moles per m$^3$ of glass melt. The very low value of physical solubility is however determined with high inaccuracy by current analytical methods. That is why we seek for new approaches to the determination of both diffusion coefficients and solubilities of gases in glass melts [6].

The goal of this work is to develop the procedure leading to the acquisition of diffusion coefficients and physical solubilities of technologically important gases in glass melts. The mathematical model of multicomponent bubble and the method of visual bubble observation in the melt are applied to acquire the above-mentioned values. The primary aim of the work is to facilitate the mathematical modeling of bubbles during melting process under real conditions.

## THEORETICAL

The kinetic equations describing the single bubble behaviour involve the term $D_i^{2/3}(m_{ib} - m_{ia}) = D_i^{2/3}(m_{ib} - L_i p_i)$ where $D_i$ is the diffusion coefficient of the i-th gas, $m_{ib}$ and $m_{ia}$ are gas concentrations in bulk glass and on the bubble surface. The quantity $L_i$ is the physical solubility of the i-th gas in the melt and $p_i$ is its partial pressure in the bubble. If the sulphate layer is present on the bubble surface, the driving force for the gas transfer can be expressed by $k(p_{SO2} p_{O2}^{1/2} - p_{SO2s} p_{O2s}^{1/2})$ where $k$ is the rate constant of the layer formation or decomposition and $p_i$ and $p_{is}$ are the partial pressure and saturation partial pressure of $SO_2$ and $O_2$ in the bubble.

Neglecting the formation of the sulphate layer, the set of equations describing the bubble behaviour at a constant temperature for $n$ diffusing gases has the form [7]:

$$\frac{da}{d\tau} = \frac{2g^2 \rho^2 a^3}{27\eta p_{ex}} + \frac{A}{p_{ex}} \sum_{i=1}^{n} \frac{D_i^{2/3}}{m_i} (m_{ib} - L_i p_i) \qquad (1)$$

$$\frac{dp_i}{d\tau} = \frac{3A}{a} \frac{D^{2/3}}{M_i} + (m_{ib} - L_i p_i) \frac{3p_i}{a} \frac{da}{d\tau} \qquad (i = 1, 2 \ldots n - 1) \qquad (2)$$

$$p_t = \sum_{i=1}^{n} p_i \qquad (3)$$

where $A = 0.382RTg^{1/3}\rho^{1/3}/\eta^{1/3}$, $a$ is the bubble radius, $p_t$ is the total pressure in the bubble, $M_i$ is the molecular mass of the i-th gas and $\rho$ and $\eta$ are glass density and viscosity.

The constant to be determined in equations (1) and (2) are $D_i$, $m_{ib}$ and $L_i$. As the mentioned quantities always occur in the form of products $D_i^{2/3}m_{ib}$ and $D_i^{2/3}L_i$, equations (1) and (2) formally involve only two unknown parameters, namely $D_i^{2/3}m_{ib}$ and $D_i^{2/3}L_i$.

The experimental measurements usually provide bubble size development $a = a(\tau)$ and bubble composition development $p_i = p_i(\tau)$. After fitting both experimental dependences by empirical functions, the derivatives $da/d\tau$ and $dp_i/d\tau$ can be obtained. If the experimental values of $da/d\tau$ and $dp_i/d\tau$ are measured for the same or at least very similar bubble, the unknown products, $D_i^{2/3}m_{ib}$ and $D_i^{2/3}L_i$, can be calculated from equations (1) and (2). In order to obtain the mentioned values, at least two experimental points must be known for both $a = a(\tau)$ and $p_i = p_i(\tau)$ dependences.

As equation (1) includes the unknown parameters of all diffusing gases, the following arrangement should be performed.

The term $1/M_i(D_i^{2/3}m_{ib} - D_i^{2/3}L_ip_i)$ is expressed from equation (2) for all gases with the exception of the gas whose properties are to be determined:

$$(D_i^{2/3} m_{ib} - D_i^{2/3} L_i p_i) = \frac{a}{3A}\left(\frac{dp_i}{d\tau} + \frac{3p_i}{a}\frac{da}{d\tau}\right) \qquad (4)$$

The values of $1/M_i(D_i^{2/3}m_{ib} - D_i^{2/3}L_ip_i$ for ($i = 1, 2\ldots n - 1$) are substituted into equation (1):

$$\frac{da}{d\tau} = \frac{A}{p_t}\left\{\sum_{i=1}^{n-1} \frac{a}{3A}\left[\frac{dp_i}{d\tau} + \frac{3p_i}{a}\frac{da}{d\tau}\right] + \frac{1}{M_i}(D_i^{2/3} m_{ib} - D_i^{2/3} L_i p_i)\right\} \qquad (5)$$

Then the appropriate form of equation (2) is:

$$\frac{dp_i}{d\tau} = \frac{3A}{aM_i}(D_i^{2/3} m_{ib} - D_i^{2/3} L_i p_i) - \frac{3p_i}{a}\frac{da}{d\tau} \qquad (6)$$

where $i$ is the index of the examined gas.

Taking into account two arbitrary chosen experimental points, namely $j$ and $j$+1, the values of the products $D_i$, $m_{ib}$ and $L_i$ (the properties of the examined gas) can be explicitly expressed by two equations. Starting from equation (6), we will get:

$$D_i^{2/3} L_i = \frac{a_{j+1}M_i}{3A(p_{i,j} - p_{i,j+1})}\left[\frac{dp_{i,j+1}}{d\tau} + \frac{3p_{i,j+1}}{a_{i+1}}\frac{da_{j+1}}{d\tau} - \frac{a_j}{a_{j+1}}\frac{dp_{i,j}}{d\tau} - \frac{3p_{i,j}}{a_{j+1}}\frac{da_j}{d\tau}\right] \qquad (7)$$

$$D_i^{2/3} m_{ib} = \frac{a_j M_i}{3A}\frac{dp_{i,j}}{d\tau} + D_i^{2/3} L_i p_{i,j} + \frac{M_i p_{i,j}}{A}\frac{da_j}{d\tau} \qquad (8)$$

As it is obvious from equation (7), the relation is applicable only when $p_{i,j} \neq p_{i,j+1}$, i.e. in the stage of developing bubble composition. To get separated values of $D_i$, $m_{ib}$ and $L_i$ from both products, one value should be obtained by another independent method. During later stages of bubble life, its composition is almost constant and the bubble growth is almost linear (bubble stationary state). Starting from equation (5) or (6) for $dp_i/d\tau$, $dp_i/d\tau = 0$ we have after integration:

$$a = a_0 + \frac{A}{p_i M_i}(D_i^{2/3} m_{ib} - D_i^{2/3} L_i p_i)\,\tau \qquad (9)$$

where $i$ is the index of the examined gas. If follows for two experimental points, $j$ and $j$+1:

$$D_i^{2/3} m_{ib} - D_i^{2/3} L_i p_{i,j} = \frac{p_i M_i}{A}\frac{a_{j+1} - a_j}{\tau_{j+1} - \tau_j} \qquad (10)$$

As it is clear from equation (10), only the value of the term $D_i^{2/3}m_{ib}$ - $D_i^{2/3}L_ip_i$ can be obtained from the arbitrary two experimental points $j$ and $j$+1 lying on curves $a = a(\tau)$ and $p_i = p_i(\tau)$. In order to obtain all three parameters, namely $D_i$, $m_{ib}$ and $L_i$, two of them should be acquired by other methods.

## Verification of the empirical procedure

The experimental dependences $a = a(\tau)$ and $p_i = p_i(\tau)$ should be replaced by empirical ones in order to get the values of appropriate derivatives, i.e. $da/d\tau$ and $d_{pi}/d\tau$. This step may be risky as the values of $da/d\tau$ and $d_{pi}/d\tau$ are very sensitive to the course of empirical functions. That is why the verification of the procedure was undertaken by using experimental tuned values of gas properties being summarized in table 1. These data were obtained from the behaviour of air and $CO_2$ bubbles.

The proposed empirical functions respecting the physical nature of bubble behaviour have the form:

$$a = (a_0 - a' - k_1\tau)\exp(-k_2\tau^{k_3}) + a' + k_1\tau \qquad (11)$$

$$p_i = (p_0 - p_{ex})\exp(-k_1\tau^{k_2}) + p_{ex} \qquad (12)$$

where $a'$, $k_1$, $k_2$ and $k_3$ are empirical constants.

The verification procedure consisted of following steps:

1. The experimental tuned values of $D_i$, $m_{ib}$ and $L_i$ were fed into the mathematical model of bubble behaviour (eqs. 1-3) and values of $da/d\tau$ and $dp_i/d\tau$ were calculated.
2. The relations $da/d\tau$ and $dp_i/d\tau$ were replaced by appropriate empirical functions (11) and (12) and the new values of $a$ and $p_i$, as well as $da/d\tau$ and $dp_i/d\tau$ were acquired as a function of time.
3. The values of products $D_i^{2/3}m_{ib}$ and $D_i^{2/3}L_i$ were calculated from equations (7) and (8) and subsequently, the values of $D_i$ and $L_i$ were acquired by using the original value of $m_{ib}$.
4. The new set of values of $D_i$, $m_{ib}$ and $L_i$ was used in the mathematical model to calculate new courses of $a = a(\tau)$ and $p_i = p_i(\tau)$.

The courses of $a = a(\tau)$ and $p_i = p_i(\tau)$ from points 1 and 4 are compared in figures 1 and 2. While the composition developments exhibit excellent agreement, the deviation between both courses of $a = a(\tau)$ dependences arises in later stages. The deviation coming from difference between original and empirical equations is acceptable up to about 600 min, i.e. longer than are bubble lifetimes under real conditions.

Table 1. The comparison of experimental tuned values of $CO_2$ and $N_2$ constants and those obtained from empirical procedure. Initial bubble compositions 100% $CO_2$ and 100% $N_2$, at 1200°C.

| | | experimental tuned values | values resulting from empirical procedure | |
|---|---|---|---|---|
| | | | 100% $N_2$ | 100% $CO_2$ |
| | $D_i$ (m$^2$/s) | $3.818 \times 10^{-14}$ | $3.430 \times 10^{-14}$ | $4.090 \times 10^{-14}$ |
| $CO_2$ | $L_i$ (kg/m$^3$ Pa) | $4.588 \times 10^{-6}$ | $4.420 \times 10^{-6}$ | $4.660 \times 10^{-6}$ |
| | $m_{ib}$ (kg/m$^3$) | $9.800 \times 10^{-2}$ | $9.800 \times 10^{-2}$ | $9.800 \times 10^{-2}$ |
| | $D_i$ (m$^2$/s) | $1.202 \times 10^{-11}$ | $1.250 \times 10^{-9}$ | $2.200 \times 10^{-11}$ |
| $N_2$ | $L_i$ (kg/m$^3$ Pa) | $1.919 \times 10^{-9}$ | $1.530 \times 10^{-9}$ | $2.490 \times 10^{-8}$ |
| | $m_{ib}$ (kg/m$^3$) | $1.500 \times 10^{-4}$ | $1.500 \times 10^{-4}$ | $1.500 \times 10^{-4}$ |

Table 2. The comparison of artificial values of $CO_2$ and $N_2$ constants and those obtained from empirical procedure. Initial bubble compositions 100% $CO_2$ and 100% $N_2$, at 1200°C.

| | | artifical values | values resulting from empirical procedure | |
|---|---|---|---|---|
| | | | 100% $N_2$ | 100% $CO_2$ |
| | $D_i$ (m$^2$/s) | $5.00 \times 10^{-13}$ | $5.08 \times 10^{-13}$ | $5.11 \times 10^{-13}$ |
| $CO_2$ | $L_i$ (kg/m$^3$ Pa) | $2.00 \times 10^{-6}$ | $1.97 \times 10^{-6}$ | $1.99 \times 10^{-6}$ |
| | $m_{ib}$ (kg/m$^3$) | $1.00 \times 10^{-1}$ | $1.00 \times 10^{-1}$ | $1.00 \times 10^{-1}$ |
| | $D_i$ (m$^2$/s) | $1.00 \times 10^{-12}$ | $0.97 \times 10^{-12}$ | $1.08 \times 10^{-12}$ |
| $N_2$ | $L_i$ (kg/m$^3$ Pa) | $1.00 \times 10^{-6}$ | $0.99 \times 10^{-6}$ | $0.99 \times 10^{-6}$ |
| | $m_{ib}$ (kg/m$^3$) | $5.00 \times 10^{-2}$ | $5.00 \times 10^{-2}$ | $5.00 \times 10^{-2}$ |

Experimentally tuned $N_2$ and $CO_2$ data however exhibit non-probable high mutual differences. Therefore we apply also the set of original artificial values estimated from the molecular size of respective gases. Table 2 illustrates that the application of the empirical procedure brings excellent values of gas constants differing from the original artificial ones within 2 %.

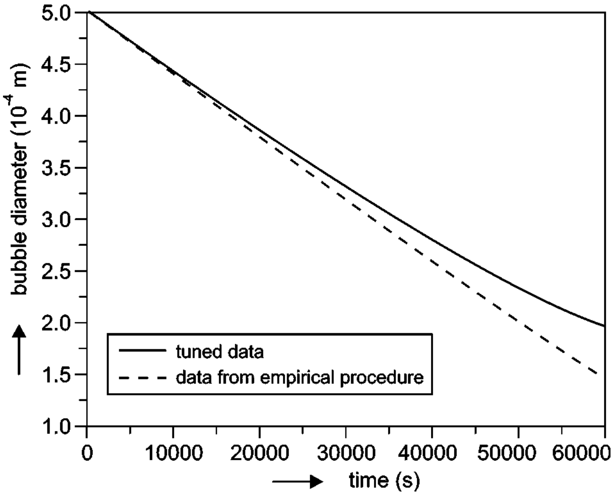

Figure 1. The comparison of courses of bubble size development using original experimental tuned data with those obtained by the empirical procedure.

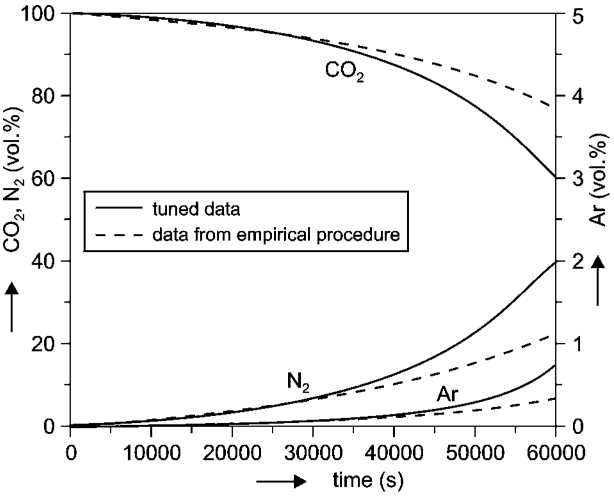

Figure 2. The comparison of courses of bubble composition developments using original experimental tuned data values with those obtained by the empirical procedure.

## EXPERIMENTAL

The method of high temperature observation of gas bubble in a glass melt was used to get the experimental dependences $a = a(\tau)$ and $p_i = p_i(\tau)$. The TV glass used for the study was prepared from dried materials of p.a. purity to get a negligible amount of chemically dissolved gases. The glass sample was inserted into a flat silica glass observation cell and heated to the measuring temperature in the laboratory furnace with an observation window. After glass melting and refining, a small bubble of defined initial composition was created by the silica glass tube with inlet of defined gas and immersed in glass. The bubble was subsequently "shuttled" in the glass melt by sucking and expelling the bubble into or out of the silica glass tube as is schematically presented in figure 3.

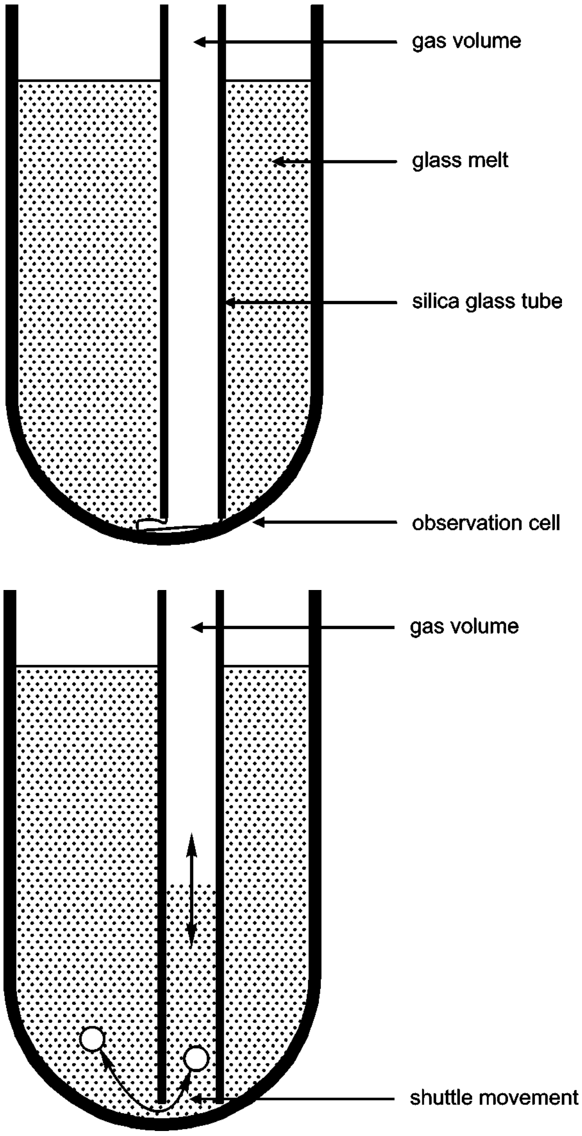

Figure 3. Scheme for the "shuttle" method.

The bubble size development was continually recorded by a digital camera. Figure 4 presents an example of a high temperature image. After finishing the experiment, the small glass sample with the examined bubble was taken out of the melt and cooled. The bubble composition was determined by mass spectrometry.

The experiments were performed with bubbles initially containing 100% Ar at temperatures 1300°C and 1400°C. The high temperature observations of bubble size development followed by the bubble composition analysis were made at each temperature for 4-7 time expositions.

## RESULTS

Figure 5 shows a typical experimental bubble size development and the course of empirical function (equation 11). As it is obvious from this figure, at least one from the couple of points necessary to calculate products $D_i^{2/3}m_{ib}$ and $D_i^{2/3}L_i$ (see equations 7 and 8)

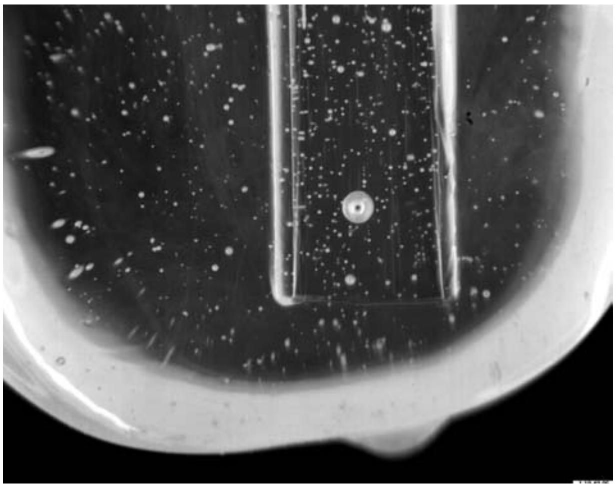

Figure 4. Micrograph of high temperature observation of a bubble in the laboratory furnace.

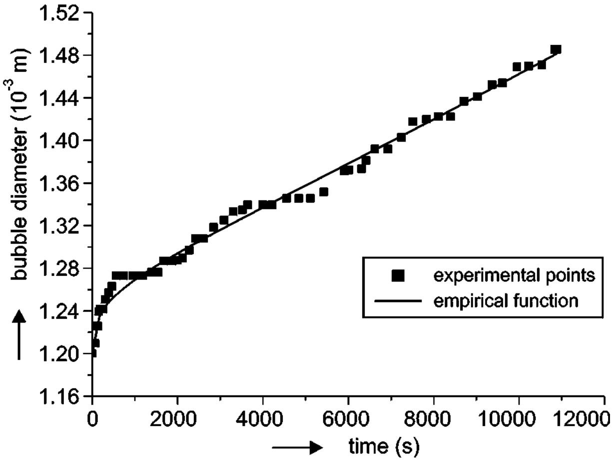

Figure 5. Experimental bubble size development and the course of the empirical function at temperature 1400°C.

should come from the time interval between 0 and about 2000 s. Another set of experimental results involved bubble analyses after finishing bubble observations at high temperatures. The experimental dependences of partial pressures of single gases on time, supplemented by empirical functions (equation 12) are presented in figure 6a-c.

The compositions of bubbles at a given time should be recalculated to the reference diameter using the equation:

$$c = \frac{d_0}{d}\, c_0 \qquad (13)$$

where $c$ and $d$ are concentration of given gas and diameter of measured bubble, and $c_0$ and $d_0$ are the same quantities relating to the reference bubble.

The values of both diameters and partial pressures as well as appropriate derivatives, namely $dd/d\tau$ and $dp_i/d\tau$, were acquired from empirical functions and the products of $D_i^{2/3}m_{ib}$ and $D_i^{2/3}L_i$ were calculated using equations (7) and (8). Table 3 presents average values of the above-mentioned products together with the standard relative deviation. The values of products were used to calculate the developments of bubble diameter and composition in time, i.e. to simulate the behaviour of experimental bubbles using the obtained data.

Figure 7 brings the comparison of experimental points and the calculated values of the bubble size at temperature 1300°C. The appropriate experimental and calculated values of bubble compositions are presented in figures 8 (1300°C) and 9 (1400°C).

Table 3. The average values of products and their standard deviation at the temperatures 1300°C and 1400°C.

| | 1300°C | |
|---|---|---|
| | $D_i^{2/3}L_i$ | $D_i^{2/3}m_{ib}$ |
| $CO_2$ | $1.41 \times 10^{-14} \pm 1.89 \times 10^{-15}$ | $1.11 \times 10^{-9} \pm 6.34 \times 10^{-11}$ |
| $N_2$ | $1.64 \times 10^{-14} \pm 2.45 \times 10^{-15}$ | $8.48 \times 10^{-11} \pm 8.87 \times 10^{-12}$ |
| Ar | $1.22 \times 10^{-14} \pm 1.17 \times 10^{-15}$ | $6.25 \times 10^{-10} \pm 7.59 \times 10^{-11}$ |
| | 1400°C | |
| | $D_i^{2/3}L_i$ | $D_i^{2/3}m_{ib}$ |
| $CO_2$ | $1.04 \times 10^{-14} \pm 7.13 \times 10^{-16}$ | $1.40 \times 10^{-9} \pm 3.08 \times 10^{-11}$ |
| $N_2$ | $2.89 \times 10^{-15} \pm 1.35 \times 10^{-15}$ | $8.72 \times 10^{-11} \pm 6.47 \times 10^{-12}$ |
| Ar | $2.56 \times 10^{-14} \pm 2.02 \times 10^{-15}$ | $1.03 \times 10^{-9} \pm 9.22 \times 10^{-11}$ |

## DISCUSSION

The values of products $D_i^{2/3}m_{ib}$ presented in table 3 increase with temperature for all examined gases. This tendency confirms the theoretical expectation. As the bulk gas concentration $m_{ib}$ is supposed independent on temperature, the increase of the product with temperature is affected by an increase of the appropriate diffusion coefficient.

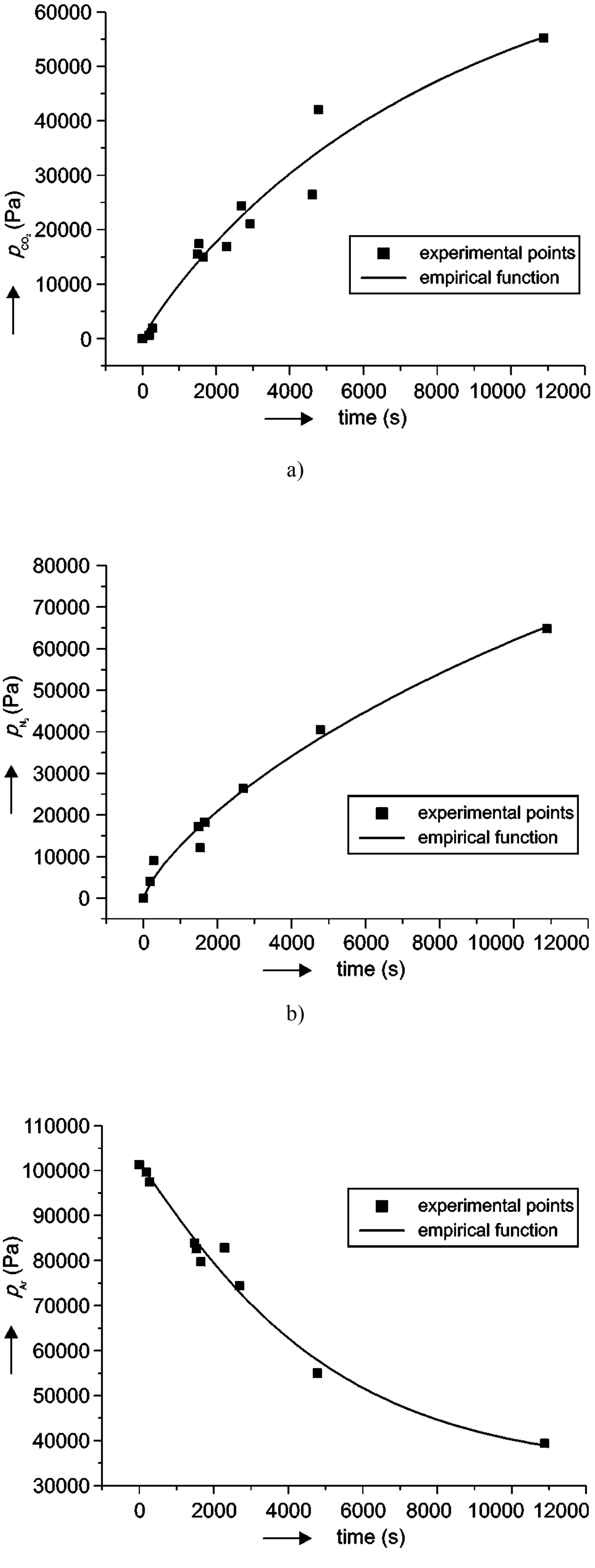

a)

b)

c)

Figure 6. The experimental bubble composition developments simulated by empirical functions at temperature 1400°C. a) $CO_2$, b) $N_2$ and c) Ar.

The product $D_i^{2/3}L_i$ may exhibit a complicated temperature dependence. In case of $CO_2$, the decrease of the product with temperature corresponds to the relatively steep decrease of $CO_2$ solubility [8]. Only physically dissolved gases, namely $N_2$ and Ar, should exhibit slight solubility increase with temperature as a consequence of thermal expansion of glass structure. However, only the argon product shows the expected temperature increase. In addition, the product $D_{N2}^{2/3}L_{N2}$ brings the highest relative experimental deviation 47 % while the same deviation for Ar and $CO_2$ is up to 10 %.

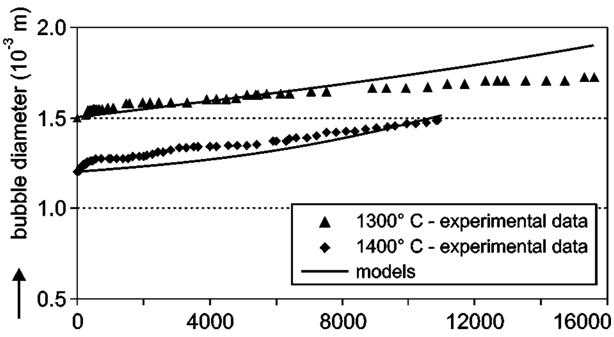

Figure 7. Experimental and calculated courses of bubble size developments at temperatures 1300°C and 1400°C.

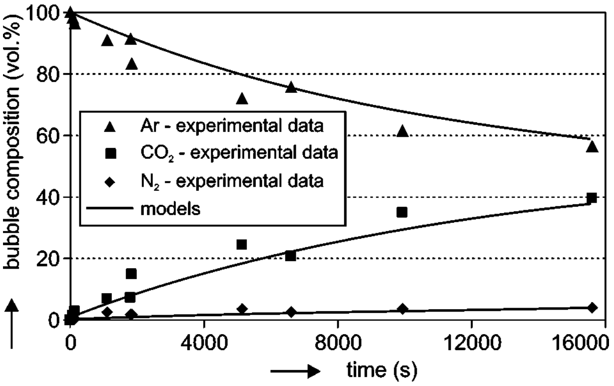

Figure 8. Experimental and calculated courses of bubble composition developments at temperature 1300°C.

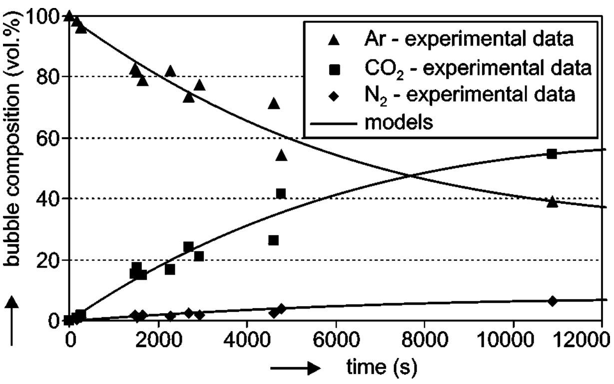

Figure 9. Experimental and calculated courses of bubble composition developments at temperature 1400°C.

Nevertheless, the use of products shows a good agreement if applied for simulation of experimental courses $p_i(\tau)$ as is obvious from figures 8 and 9. The comparison of bubble size developments, obvious from figure 7, shows a growing deviation of the model from the experiment; however, the relative error after 15600 s did not exceed 10 %. Thus, the values of products appear suitably precise for the mathematical simulation of bubbles. This fact facilitates the mathematical modeling of bubbles sources under real conditions with an acceptable precision.

As it was mentioned in the Theoretical, separated values of gas properties $D_i$, $m_{ib}$ and $L_i$ can be obtained from corresponding products when one gas quantity is acquired by another independent method. In this study, the measured values of $CO_2$ bulk concentration and estimated quantities of Ar and $N_2$ were applied [8].

Unfortunately, only values for $CO_2$ may be considered to correspond to the real ones. The gas solubility of tenths of mols per $m^3$ of glass is a rasonable value, as well as the values of the diffusion coefficient when comparing them with corresponding values in float glass [8]. However, the only estimated actual concentrations of both Ar and $N_2$ in the melt devaluated the appropriate values of diffusion coefficients and solubilities. As is obvious from table 4, especially the values of $D_{Ar}$ are too high and $L_{Ar}$ too low with respect to the expected values. The more reliable procedure is therefore needed to determine one of three quantities by an independent method. As gas solubilities in glass melts differ much less than their bulk concentrations in glass, the physical solubility measurement may become the required independent measurement.

Table 4. The calculated values of $CO_2$, $N_2$, Ar properties and experimentally obtained bubble growth rates $da/d\tau$ at the temperatures 1300°C and 1400°C.

| | | 1300°C | 1400°C |
|---|---|---|---|
| | $D_i$ ($m^2$/s) | $1.20 \times 10^{-12}$ | $1.70 \times 10^{-12}$ |
| $CO_2$ | $L_i$ (kg/$m^3$ Pa) | $1.24 \times 10^{-6}$ | $7.79 \times 10^{-7}$ |
| | $m_{ib}$ (kg/$m^3$) | $9.80 \times 10^{-2}$ | $9.80 \times 10^{-2}$ |
| | $D_i$ ($m^2$/s) | $4.27 \times 10^{-10}$ | $4.44 \times 10^{-10}$ |
| $N_2$ | $L_i$ (kg/$m^3$ Pa) | $2.89 \times 10^{-8}$ | $4.82 \times 10^{-9}$ |
| | $m_{ib}$ (kg/$m^3$) | $1.50 \times 10^{-4}$ | $1.50 \times 10^{-4}$ |
| | $D_i$ ($m^2$/s) | $4.44 \times 10^{-8}$ | $9.40 \times 10^{-8}$ |
| Ar | $L_i$ (kg/$m^3$ Pa) | $9.81 \times 10^{-10}$ | $1.24 \times 10^{-9}$ |
| | $m_{ib}$ (kg/$m^3$) | $5.00 \times 10^{-5}$ | $5.00 \times 10^{-5}$ |
| | $da/d\tau$ (m/s) | $5.04 \times 10^{-9}$ | $1.11 \times 10^{-8}$ |

## CONCLUSIONS

The procedure based on the experimental measurement of bubble size and composition developments was used for the acquisition of diffusion coefficients, solubilities and bulk concentrations of $CO_2$, $N_2$ and Ar in TV glass at temperatures 1300°C and 1400°C.

The presented results show that the applied method of artificial bubbles is usable for the mathematical simulation of bubbles in melts, but another independent and sufficiently precise method is missing to get sufficiently true values of physical gas constants in glass melts, namely their diffusion coefficients, solubilities and actual concentrations in the melt.

The question arises about the applicability of the mentioned procedure for other technologically important gases, i.e. $O_2$, $SO_2$ and $H_2O$. This is an object of authors' next effort.

## Acknowledgement

*This work was supplied with the subvention by the Grant Agency of ASCR, Project No. S4032103 and by the Ministry of Education, Youth and Sports of the Czech Republic, Project No. MSM 223100002.*

## References

1. Doremus R. H.: J.Am.Ceram.Soc. *49*, 461 (1966).
2. Němec L., Kloužek J.: Ceramics-Silikáty *39*, 1 (1995).
3. Doremus R. H.: *Glass Science*, p.122, John Wiley & Sons Inc., New York 1994.
4. Perkins W. G., Begael D.R.: J.Chem.Phys. *54*, 1683 (1971).
5. Norton F. J.: Nature *191*, 701 (1961).
6. Ramos J. I.: J.Am.Ceram.Soc. *69*, 149 (1986).
7. Němec L., Kloužek J.: Ceramics-Silikáty *47*, 81 (2003).
8. Kloužek J.: Unpublished results

---

## KINETICKÁ A ROVNOVÁŽNÁ DATA PLYNŮ V ROZTAVENÝCH SKLECH

MARCELA JEBAVÁ, LUBOMÍR NĚMEC, JAROSLAV KLOUŽEK

*Laboratoř anorganických materiálů,*
*společné pracoviště Ústavu anorganické chemie AV ČR a*
*Vysoké školy chemicko-technologické v Praze*
*Technická 5, 166 28 Praha*

Metoda vysokoteplotního sledování s následnou analýzou bublin hmotnostní spektrometrií byla použita pro stanovení vlastností plynů v roztavených sklech. Metoda vychází z matematického modelu chování bublin v tavenině simulujícího časový vývoj jejich rozměru a složení. Obě závislosti byly experimentálně měřeny a využity ke stanovení difúzních koeficientů, rozpustností a aktuálních koncentrací $CO_2$, $N_2$ a Ar ve skle pro televizní obrazovky při teplotách 1300°C a 1400°C.